Available on CMS information server

**CMS CR -2011/051**

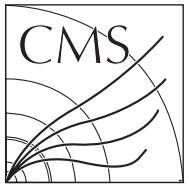


**The Compact Muon Solenoid Experiment**

**Conference Report**

Mailing address: CMS CERN, CH-1211 GENEVA 23, Switzerland


**28 April 2011 (v2, 09 May 2011)**

# CMS trigger and data taking in 2010

Malgorzata Kazana for the CMS Collaboration

**Abstract**

The Compact Muon Solenoid (CMS) detector is a general purpose experiment at the Large Hadron Collider (LHC) accelerator. The CMS trigger performance with proton-proton collisions during the first year of the LHC's operation in 2010 is presented. The CMS trigger system is also described and trigger efficiency results and selected applications for physics analyses are presented.

Presented at *Epiphany 2011: Cracow Epiphany Conference on the First Year of the LHC*

# CMS trigger and data taking in 2010*

Małgorzata KAZANA

*on behalf of the CMS Collaboration*
Soltan Institute for Nuclear Studies, Hoża 69, 00-689 Warsaw, Poland

The Compact Muon Solenoid (CMS) detector is a general purpose experiment at the Large Hadron Collider (LHC) accelerator. The CMS trigger performance with proton-proton collisions during the first year of the LHC's operation in 2010 is presented. The CMS trigger system is also described and trigger efficiency results and selected applications for physics analyses are presented.

## 1. First year of the CMS experiment data taking

The year 2010, was the first year of the LHC operation. Proton beams reached a new energy region of $3.5\,TeV$, and lead ions were injected for the first time into the LHC's beams. All the objectives of the LHC machine have been achieved. A peak in the instantaneous luminosity of $2 \times 10^{32} cm^{-2} s^{-1}$ was reached in $pp$ collisions. Since then, the amount of collected data was doubled in only a few days as shown in Fig. 1a. The CMS experiment accumulated $43\,pb^{-1}$ of $pp$ data. During LHC operations CMS has obtained a high data taking efficiency of 92 %. The main source of data taking inefficiency was the procedure of switching on all sub-detectors, which have to remain off due to safety reasons, before stable beam condidtions hads been declared by the LHC's machine team. During four weeks of heavy lead ion collisions at $2.76\,TeV$ nucleon-nucleon centre-of-mass energy per nucleon pair, CMS recorded about $8\,\mu b^{-1}$ of $PbPb$ data with the overall data recording efficiency of 93 %. The data taking performance of the CMS experiment during $PbPb$ collisions is illustrated in Fig. 1b.

The CMS trigger has worked according to specifications and has delivered good quality data for analysis.

* Presented at Cracow Epiphany 2011 Conference

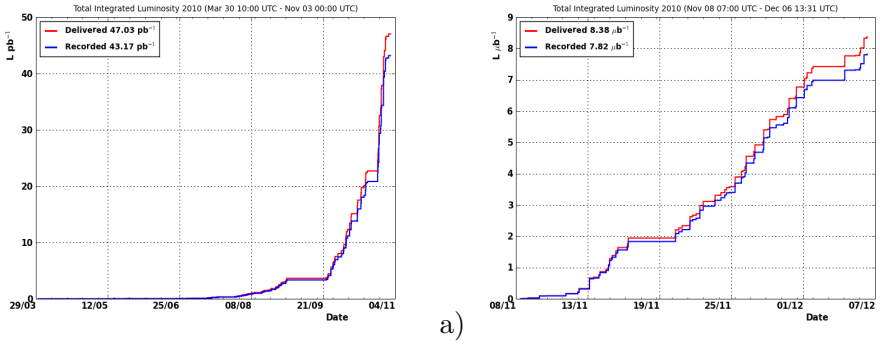


a) b)

Fig. 1. The CMS data taking performance in 2010. Integrated luminosity versus time delivered to (red), and recorded by CMS (blue) during (a) $pp$ stable beams at $7\,TeV$ centre-of-mass energy and (b) $PbPb$ stable beams at $\sqrt{s_{NN}} = 2.76\,TeV$.

## 2. CMS trigger architecture

The LHC was built to study the origin of the electroweak symmetry breaking and Beyond Standard Model physics. The most interesting events are rare and have to be found in the bulk of QCD events. Therefore, the trigger is a key element of the data taking system. The design rate of $pp$ events is $40\,MHz$. Therefore the electronics frequency chosen for the trigger system has the same baseline frequency. The $40\,MHz$ rate is too high to store all the data from collisions. For one event, about $1\,MB$ of data has to be recorded. The disk storage capability is limited to the order of $\mathcal{O}(100)\,MB/s$ which means that 100-300 events can be registered per second with a rate of $\mathcal{O}(100-300)\,Hz$. The aim of the trigger system is to reduce event rate by 5 orders of magnitude without rejecting any interesting events.

The CMS trigger system is divided in two levels. The scheme of the trigger is shown in Fig. 2a. The first level delivers a quick decision based on the information from hardware elements. In the second level the full event is analyzed to decide if the event should be accepted for storage on disk.

The first level (L1) of the CMS trigger system [1] uses information from the calorimeters and muon detectors to select (in less than $3.2\,\mu$s, equal to the length of electronic buffers) the most interesting events. The calorimeter trigger works on primitives from two sub-detectors: the electromagnetic calorimeter (to build electron and photon candidates) and the hadron calorimeter (which allows to trigger on jets). Details of the Level-1 architecture are presented in Fig. 2b. The L1 muon trigger receives signals from three muon systems based on hits detected in Drift Tubes or Cathode Strip Chambers and Resistive Plate Chambers (RPC). The main goal of

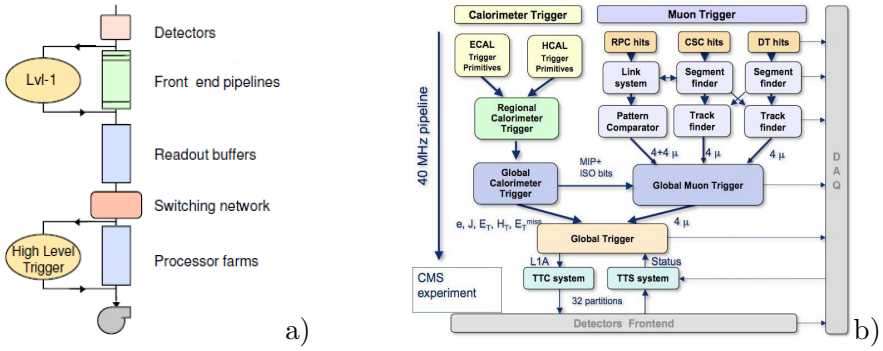


Fig. 2. The CMS trigger architecture: (a) the general scheme and (b) the L1 scheme.

the L1 trigger is to provide a list of the most energetic candidates from different classes, e.g.: $4\,e/\gamma$, $4\,\mu$, 4 jets or MET (missing transverse energy). Additionally, technical triggers, which analyzes signals from LHC beam counters and CMS beam scintillators are deployed. Up to 128 physical algorithms and 64 technical ones are used to evaluate the final L1 decision taking into account other requirements, such as trigger rules (e.g. no more than one L1 Accept per $75\,ns$) or pre-scaling (only a fraction of events that fulfill given conditions is accepted). The L1 trigger reduces rates from $40\,Mz$ to $100\,kHz$.

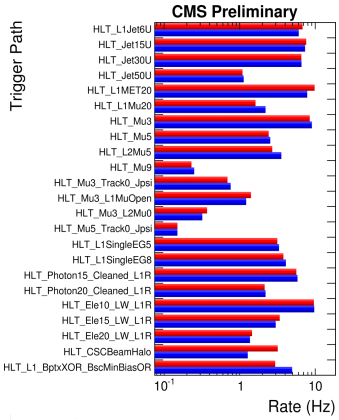


Fig. 3. Trigger rates extrapolated from data. Red bins denote measured rates during data taking at the instantaneous luminosity $\mathcal{L} = 4.6 \times 10^{29}\, cm^{-2} s^{-1}$, whereas blue bins represent extrapolated rates measured at $1 \times 10^{29}\, cm^{-2} s^{-1}$ and scaled by a factor of 4.6.

The High Level Trigger (HLT) [2] code is run on a large processor farm which further decreases the event rate to $300\,Hz$ before data storage. The HLT software evaluates up to 150 trigger paths using full granularity data. Its internal sub-structure has rising complexity and flexibility. At the last stage, the HLT subdivides processed data into data streams with respect to physics, calibration and data quality requirements. The average

time of the HLT calculations for one event is $40\,\mu s$. There are enough adjustment possibilities to change algorithms in order to keep the HLT timing at this level in the future. For comparison, the full and detailed reconstruction of a proton-proton event takes about $2\,s$. In 2010, the CMS operation was continuously adapted to the LHC conditions by customizing the trigger menu. In the low luminosity regime, the trigger decision was based on simple threshold cuts, for higher luminosities, thresholds were higher and more elaborated algorithms were used. New trigger menus were prepared for each twofold increase in luminosity. It was possible to predict future rates using current rates. An example is shown in Fig. 3. A fairly linear behaviour between extrapolated and predicted rates was observed.

One of the main goals of the trigger is a proper assignment of events to the bunch crossing it originated from. Therefore, data have to be synchronized with the LHC clock every $25\,ns$ by taking into account different sources of delays, such as geometrical delays, the time for signal propagation or electronics jitter. All CMS sub-detectors had performed the synchronization procedure during start-up of the LHC. As an example, the results of the RPC trigger synchronization are shown. The RPC trigger synchronization was in a very good stage and 99.9 % of the RPC hits had a proper time assignment, as shown in Fig. 4a. As a consequence, the RPC trigger provided its answer in the expected bunch crossing and any pre-triggers with respect to the L1 accepted signal were practically not observed, as illustrated in Fig. 4b.

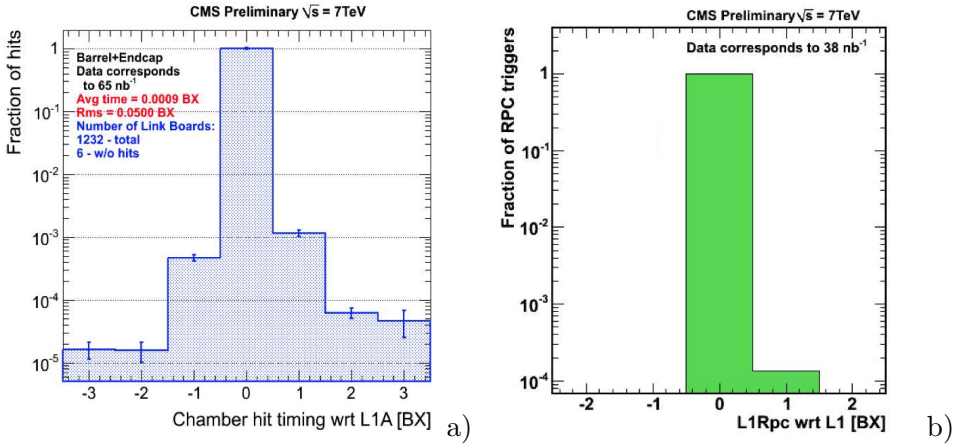


Fig. 4. The RPC system synchronization. The timing of the RPC chamber hits (a) and RPC triggered muons (b) with respect to timing of the L1 trigger given in bunch crossing units ($1BX = 25\,ns$).

## 3. Trigger efficiency results

During 2010 data taking, CMS worked with event rates of the order of about $70\,kHz$ at L1 and between 300-600 $Hz$ output rate at the HLT. All sub-systems of the trigger had verified their performance.

A common way to evaluate the efficiency of a trigger is to check the threshold efficiency, which is the probability that for a reconstructed muon with transverse momentum $p_T$, the trigger algorithm assigns to this muon a momentum greater or equal to the threshold value, $p_T^{CUT}$. It is expected that the trigger efficiency should reach a plateau closely to the threshold value. The trigger efficiency curve is the so-called a *turn-on curve*. A steep beginning of the curve, a high value of the efficiency at the nominal threshold cut and a plateau level near 100 % confirms a good performance of the trigger.

The trigger efficiency can be evaluated with events selected by minimum bias triggers. Those triggers are based on the Beam Pick-up Timing for the eXperiments (BPTX) monitors and Beam Scintillator Counters (BSC). The positions with respect to the nominal CMS are schematically drawn in Fig. 5. Two BPTX monitors are positioned symmetrically on both sides of CMS,

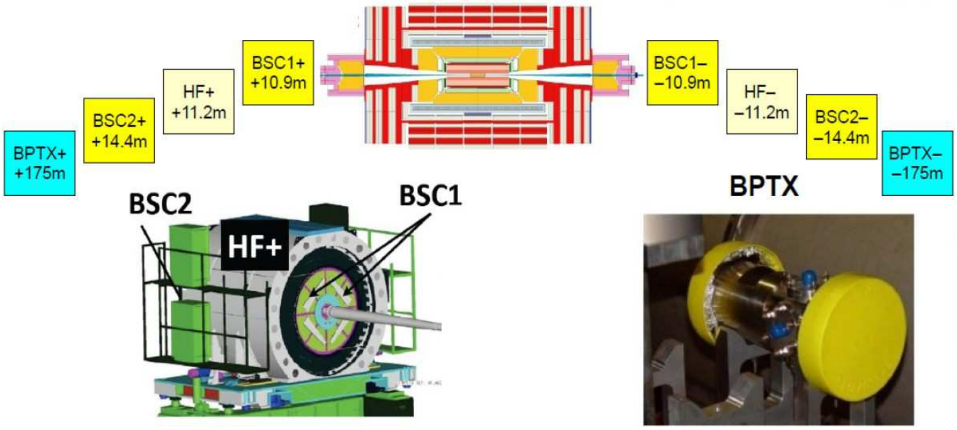


Fig. 5. Minimum bias trigger detectors in the CMS experiment.

$175\,m$ from the center of the detector. They provide precise information about the structure and timing of incoming beams with a resolution of $0.2\,ns$. BSCs are positioned on the Hadron Forward (HF) Calorimeters outside of the CMS endcaps. The minimum bias trigger is accepted if a coincidence of signals is present in the BSCs or BPTXes. This trigger gave an opportunity to study soft physics without pileup in the initial phase of the LHC with luminosities $(10^{28} - 10^{31})\,cm^{-2}s^{-1}$ and selected unbiased events for trigger performance studies.

A tag-and-probe method is a powerful tool to measure the trigger efficiency from data. In this method, a mass resonance particle decaying to a pair of electrons of muons is used to select lepton pairs to probe the efficiency of a particular selection criterion. Usually, the $J/\psi$ particle is used for low momentum leptons and the $Z$ boson is used for checking a wider spectrum of leptons. A tag particle is defined as a lepton passing a very tight selection, with very low fake rate ($\ll 1\,\%$). A probe particle is a lepton passing softer selection. It is paired with a tag object in a way that the invariant mass of tag-and-probe combination is consistent with the resonance mass. The resulting trigger efficiency is then the ratio of a number of probes passing the selection criteria and a total number of probes counted using the resonance.

### *3.1. Muon trigger*

At the L1 trigger stage, up to four muon candidates are provided by the system based on DT and CSC and RPC chambers. The L1 muons are produced by the track finder of the CSC and DT trigger systems. The RPC, which is a trigger-dedicated sytem, works in a different way. A pattern comparator (PAC) is implemented in the trigger electronics. It provides a good time resolution ($\sim ns$). Muons crossing the detector fire strips in up to six or three layers of RPCs in the barrel or endcaps respectively. The pattern left by a muon is compared with previously defined patterns for a given transverse momentum and location in the detector. The use of PAC guarantees a correct bunch crossing identification.

The local muon trigger performance during 2010 data taking was evaluated in terms of efficiency [3] and it is shown in Fig. 6 for the CSC and DT trigger systems and Fig. 7 for the RPC trigger. The tag-and-probe method using $J/\Psi \to \mu^+\mu^-$ was applied in the DT trigger efficiency anal-

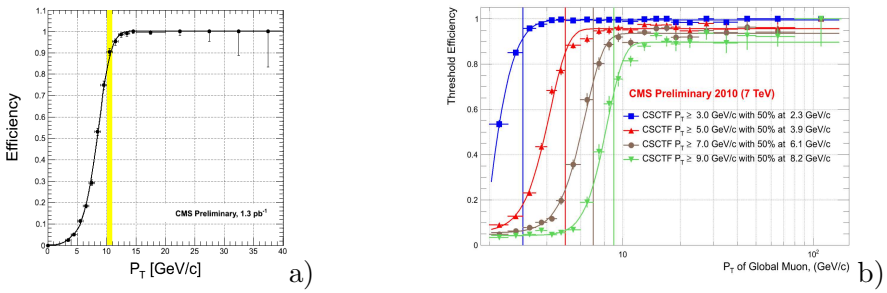


Fig. 6. The L1 muon trigger system performance as a *turn-on curve*. (a) For the DT system in the $|\eta| < 1.1$ region for $p_T^{CUT} = 10\,GeV/c$. (b) For the CSC system in $1.2 < |\eta| < 2.1$.

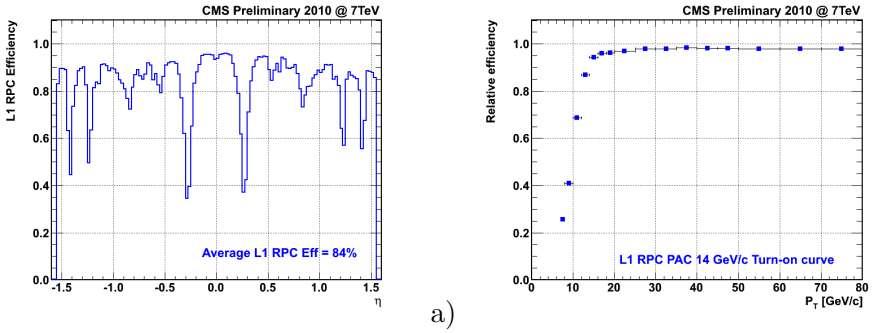


Fig. 7. a) The L1 RPC trigger efficiency including detector geometrical acceptance and the hit efficiency for reconstructed muons with $p_T > 7\,GeV/c$ if the L1 CSC or DT trigger was fired. b) The L1 RPC *turn-on curve* for $p_T^{CUT} = 14\,GeV/c$ with the same conditions for muons.

ysis. In analyses for CSCs and RPCs, all reconstructed muons were considered. Muons triggered only by a given system itself were not taken into account. The *turn-on curve* present a very good performance of the muon triggers. However, the absolute trigger efficiency depends also on the detector geometrical acceptance and the hit efficiency, as it is shown for the RPC trigger in Fig. 7a. In 2010, the RPC algorithm required four of six fired layers for the muon candidates in the barrel and all three fired layers in the endcaps. In order to reduce inefficiency, the RPC trigger algorithm was changed in 2011 and three fired layers were required to build patterns in the barrel.

At the level of the L1 Global Muon Trigger (GMT), where information from all muon sub-systems is merged, detector acceptance inefficiencies are significantly reduced. Already, during the first months of data taking at the LHC start-up, when the whole CMS detector was not yet ideally aligned and synchronized, the global L1 trigger efficiency was above 95 % in the barrel and close to 100 % in the endcaps for low transverse momentum muons from the minimum bias events (Fig. 8a). The efficiency in the endcaps was better in data than in the full detector simulation because of the special settings of the CSC for the low intensity proton beam.

The final decision of the L1 GMT is transmitted to the software based HLT, where all hits in the muon chambers are refitted with the full granularity of the detector. The muon track reconstruction is done in the L1 region of interest. Finally, muon tracks are matched to the tracker trajectories and a better measurement of their transverse momentum is obtained. The HLT muon trigger efficiency is presented for the low transverse momentum muons from minimum bias events with the first LHC data on Fig 8b. The efficiency in data was lower than in the simulated data because of the

preliminary synchronization of the muon detector.

### *3.2. Calorimeter trigger*

The electromagnetic (ECAL) and hadron (HCAL) calorimeters have been designed to precisely measure energies of photons, electrons and jets. Triggers based on the calorimeter are used for selecting interesting physics events.

At L1, the trigger decision is based on local energy deposits called trigger primitives, which refer to single trigger towers. A trigger tower is a well defined unit of the calorimeter with projective geometry followed from the ECAL to the HCAL, i.e. a matrix of $5 \times 5$ lead tungstate crystals of the ECAL corresponds to the size of a HCAL trigger tower. The front-end electronics perform a computation of trigger primitives by summing the transverse energy deposited in the tower. The information about ECAL and HCAL primitives is sent to the Regional Calorimeter Trigger, where implemented algorithms combine trigger primitives into Level-1 trigger candidates. In the next step, candidates form all regions and classes (e.g.: $e/\gamma$, jets) are sorted according to their transverse energy by the Global Calorimeter Trigger, and only the most energetic four are sent to the Global Trigger, which generates the final decision (L1 accept) based also on L1 muon triggers.

The $e/\gamma$ and jet triggers consist of different paths with configurable thresholds for calorimeter energy deposits. The L1 electron or photon candidate has to pass a minimal transverse energy cut $E_T^{CUT} = 5\,GeV$ to be accepted by the trigger path *L1_SingleEG5* or the L1 jet with $E_T^{CUT} = 20\,GeV$ to be accepted by the trigger path *L1_SingleJet20U*.

The performance of jet trigger was evaluated on events selected on minimum bias trigger. Additionally, a standard filtering and cleaning for noise and anomalous signals in the HCAL was required. In the offline jet re-

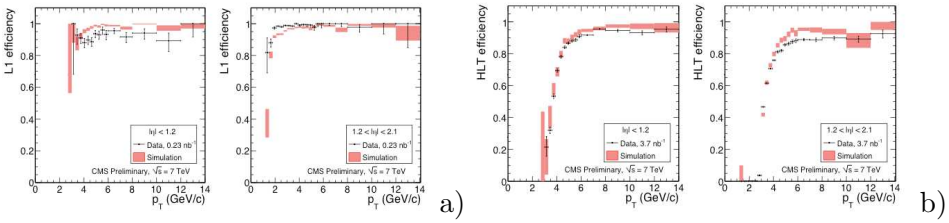


Fig. 8. The muon trigger performance at the start-up of the LHC. The L1 (a) and HLT (b) muon trigger efficiency for minimum bias events in $pp$ collisions. Efficiency plots are for low momentum muons with $p_T > 3\,GeV/c$ and presented separately for barrel $|\eta| < 1.2$ and endcaps $1.2 < |\eta| < 2.1$.

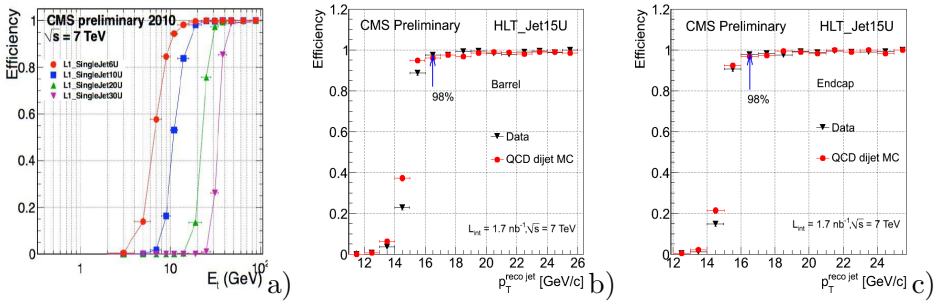


Fig. 9. The jet trigger performance: the L1 (a) and HLT (b,c separately for the barrel and endcaps) jet trigger efficiencies for hadron calorimeter trigger paths pointed out in the legend of plots.

construction, the *anti-$k_T$* interactive cone jet algorithm with a cone size $\triangle R = 0.5$ was used. The same algorithm is used for finding jet candidates at the HLT. Additionally, a loose jet identification was required in the pseudo-rapidity range $|\eta| < 2.6$. In order to calculate the trigger efficiency, the leading offline jet was matched to a L1 jet if $\triangle R < 0.5$. The results for different L1 jet triggers are shown in Fig. 9a. The L1 trigger efficiency reaches 100 % plateau with a sharp *trun-on curve*. The HLT jet performance was compared with Monte Carlo (MC) simulations of the QCD dijet events. Data events were selected by the unbiased open muon triggers. HLT jets were required to mach offline jets with the condition of $\triangle R < 0.1$. Data and MC events are consistent and the *HLT_Jet15U* trigger is 100 % efficient above $p_T^{reco\ jet} = 18 GeV/c$ (Figs. 9b,c).

At the HLT, $e/\gamma$ objects are reconstructed using seeds from the L1. In the first step L1 candidates are spatially matched to ECAL clusters, from which the super-clusters are formed. The transverse energy cut is applied and calorimetric (ECAL and HCAL) isolation is verified. In the next step, HLT photons are distinguished from HLT electrons. If no pixel track matches an ECAL super-cluster, a tight track isolation is required for photons, in contrast to electrons, for which loose track isolation in a *hollow* cone is checked.

As an example of the HLT $e/\gamma$ algorithm, the efficiency of the HLT photon trigger with $E_T^{CUT} = 15\, GeV$ was evaluated. Events from minimum bias triggers with a significant activity in the ECAL and reconstructed offline super-clusters were used as tags to probe the production of *HLT_Photon15* triggers. In this case, the efficiency of the trigger path is equal to the ratio of the number of events firing this trigger path and the total number of events, as it is shown in Fig. 10a. In Fig. 10b the efficiency is calculated with respect to the L1 trigger. The very good calorimeter trigger performance is

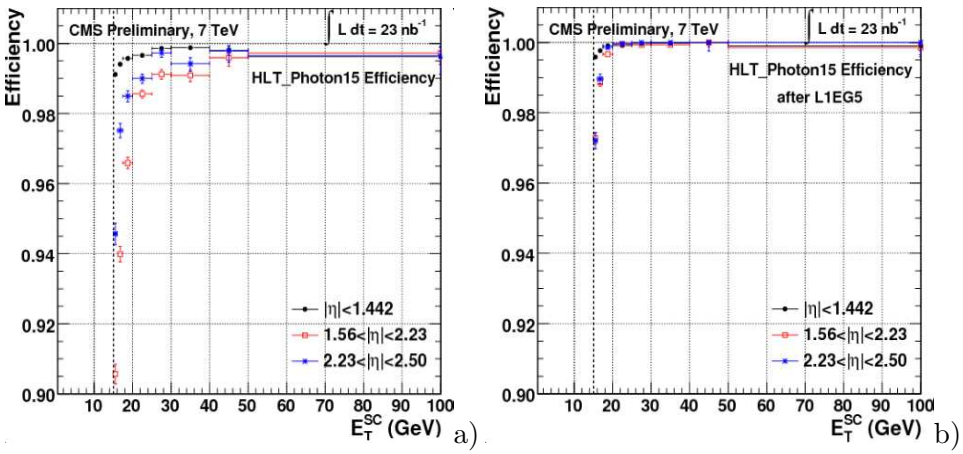


Fig. 10. The calorimeter trigger performance at the start-up of the LHC. The efficiency of the photon trigger with $E_T^{CUT} = 15\,GeV$ (a) w.r.t. events triggered by the minimum bias trigger with a significant activity in the ECAL or (b) w.r.t. the same events which passed the L1 $e/\gamma$ condition with $E_T^{CUT} = 5\,GeV$.

again confirmed [4].

The use of the tag-and-probe method allows to make a comparison with the MC data. The Z$\rightarrow$ $e^+e^-$ mass resonance was used for evaluation of the electron trigger efficiency during the high (in 2010) luminosity regime, $10^{31}\,cm^{-2}s^{-1}$. Fig. 11 shows the good agreement for the electron trigger

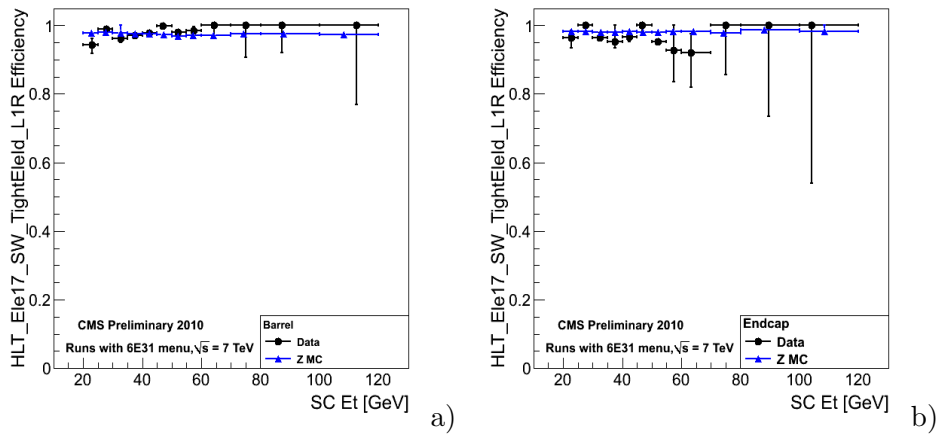


Fig. 11. The HLT efficiency for the electron trigger path ($E_T^{CUT} = 17GeV/c$ with tighter calorimeter-based electron identification and isolation) for (a) the barrel and (b) endcaps of the CMS detector.

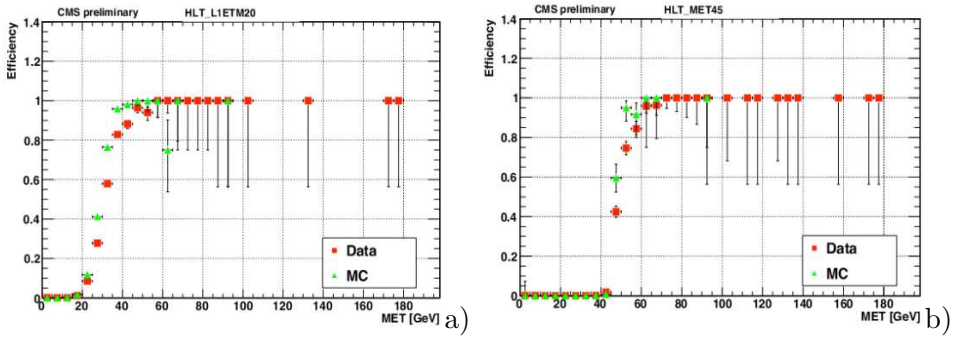


Fig. 12. The efficiency for the offline calorimetric MET object to pass the HLT trigger: (a) MET>25$GeV$ if L1$^{\mathrm{JET}}$>6$GeV$ or (b) MET>45$GeV$ if L1$^{\mathrm{JET}}$>20$GeV$. The data-set corresponds to 11 $pb^{-1}$ of $pp$ data. MC simulation is for QCD events with jets above $p_T > 15\,GeV/c$.

path efficiencies for data and the MC data. The efficiency reaches 100 % within errors.

At the level of HLT, the missing transverse energy (MET) object is also created. The MET is determined from the transverse vector sum over energy deposits in the calorimeter towers. The HLT MET path efficiency was evaluated for the reconstructed offline MET variable. The two distributions in Fig. 12 are in a good agreement between data and MC simulations. The resolution of the reconstruction of MET is worse than the reconstruction resolution of electrons, muons and jets separately. Therefore the MET efficiency curves reach the 100 % plateau at higher values than it was shown for other trigger variables.

## 4. Trigger applications

The CMS experiment used dedicated triggers to search for new phenomena in 7$TeV$ center-of-mass energy $pp$ collisions.

The CMS experiment looks for evidence of long-lived particles that stop in the detector and decay in the quiescent periods between beam crossings [5]. New heavy quasi-stable particles were present in many Beyond the Standard Model processes [5]. CMS has targeted gluinos from split supersymmetry with relatively large cross sections at the LHC. Decays of gluinos, $\tilde{g} \rightarrow g + \tilde{\chi}_1^0$, are suppressed due to heavy squarks masses. These gluinos hazdronize into charged or neutral states called R-hadrons and may stop anywhere inside the CMS detector with a probability of about 20 % according to the so-called cloud model of electromagnetic and nuclear integrations of R-hadrons with matter [6]. The lifetime of R-hadrons is not known, but is expected to be longer than an average time needed by a rel-

ativistic particle to cross the detector. R-hadrons may decay after seconds, minutes or days producing jet-like objects, depositing energy in the CMS calorimeters. Detection of these particles requires a special trigger, which has to work at times when there are no collisions, in contrast to standard procedures. In CMS, a dedicated jet-trigger based on the hadron calorimeter was designed. Additionally, the condition that the trigger must not fire on jets produced in $pp$ collisions is fulfilled by using information from the BPTX monitors. The L1 trigger requires a jet with at least $10\,GeV$ transverse energy. A $20\,GeV$ threshold on jet energy is applied in the HLT. At both L1 and HLT, the pseudo-rapidity of the jet, $|\eta_{jet}|$, is required to be less than 3.0. Measured rates of events were about $90\,Hz$ at L1 and $3.3\,Hz$ at HLT.

Several beam-related processes remain possible sources of background and have to be rejected during further data analysis. In order to reject background events due to an unpaired proton bunch passing through CMS, events in which either BPTX is over threshold are vetoed. Instrumental effects during trigger generation, and features of the LHC beam such as lower intensity satellite bunches that accompany the colliding protons, can cause triggers in some of the $25\,ns$ ($BX$) intervals which precede or follow the one in which the intended proton collisions occur. Therefore any event occurring up to two $BX$s before, or one $BX$ after, the $BX$ in which collisions are expected, are rejected. To remove beam-halo muon events, which may not be synchronous with proton collisions, a loose beam-halo veto using the CSC in the endcap muon system is used. The algorithm rejects events in which a beam-halo trigger was recorded, or a track segment was reconstructed in the CSC system with timing consistent with beam-halo, or a muon track was reconstructed with beam-halo-like kinematics.

Finally, to ensure that no out-of-time $pp$ collision events due to satellite bunches contaminate the search sample, events with one or more reconstructed primary vertices are rejected. Additional sources of background are cosmic muons which may deposit a significant amount of energy in the calorimeters. To reduce this background, events that contain reconstructed muons are vetoed. The instrumental noise is removed by restricting jet requirements. In order to suppress noise fluctuations and energy deposits from cosmic rays in calorimeters, only jets with reconstructed

| Lifetime [s] | Expected Background ($\pm$ stat. $\pm$ syst.) | Observed |
|---|---|---|
| $1 \times 10^{-7}$ | $0.8 \pm 0.2 \pm 0.2$ | 2 |
| $1 \times 10^{-6}$ | $1.9 \pm 0.4 \pm 0.5$ | 3 |
| $1 \times 10^{-5}$ | $4.9 \pm 1.0 \pm 1.3$ | 5 |
| $1 \times 10^{6}$ | $4.9 \pm 1.0 \pm 1.3$ | 5 |

Fig. 13. Search for stopped gluinos in $pp$ collisions: number of observed counts and background predictions for selected values of gluino lifetimes.

energies above $50\,GeV$ are accepted. Additionally, it is required that the leading jet has to be located in the central part of the detector for $|\eta_{jet}^{1st}| < 1.3$ and must have 60 % of its energy contained in fewer than 6 towers.

The signal simulation was done using customized versions of the PYTHIA event generator and the GEANT4 particle interaction simulator. Gluino masses in the range 150 to $500\,GeV/c^2$ were studied.

A counting experiment was performed for the gluino lifetime hypotheses from $75\,ns$ to $10^6$ seconds, where the upper limit was the longest lifetime for which at least one event still could be observed. The results of this counting experiment for selected lifetime hypotheses are presented in Fig. 13.

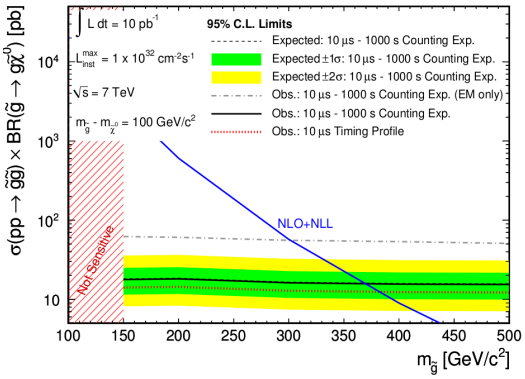


Fig. 14. 95 % C.L. limits on gluino pair production cross section times branching fraction as a function of gluino mass assuming the cloud model of R-hadron interactions (solid line) and EM interactions only (dot-dashed line). Results are presented for $m_{\tilde{\chi}_1^0} > 50\,GeV/c^2$.

No significant excess above background was observed in the search sample with a peak instantaneous luminosity of $1 \times 10^{32} cm^{-2} s^{-1}$, an integrated luminosity of $10\,pb^{-1}$, and a search interval corresponding to 62 hours of LHC operation. In the absence of any discernible signal, the 95 % confidence level (C.L.) limits over 13 orders of magnitude in gluino lifetime using a hybrid CLS method were set. For a mass difference $m_{\tilde{g}} - m_{\tilde{\chi}_1^0} > 100\,GeV/c^2$, assuming $\mathrm{BR}(\tilde{g} \to \tilde{\chi}_1^0) = 100\,\%$, CMS was able to exclude lifetimes from $75\,ns$ to $3 \times 10^5\,s$ for $m_{\tilde{g}} = 300\,GeV/c^2$ with the counting experiment. The result as a function of the gluino mass is presented in Fig. 14. Under the same assumptions as for the cross section limit, gluino masses below $m_{\tilde{g}} < 370\,GeV/c^2$ are excluded for lifetimes between $10\,\mu s$ and $1000\,s$. These results are the most restrictive to date and extend previous limits from the D0 Collaboration on both gluino lifetime and gluino mass.

## 5. Conclusion

The performance of the L1 and HLT triggers was evaluated in terms of efficiency. The trigger efficiencies of all trigger systems presented sharp *turn-on curves* in good agreement with simulations. The CMS trigger menus

successfully accommodated the increase of the LHC luminosity corresponding to the requirements for the physics analyses.

## 6. Acknowledgment

This work was supported in part by Polish Ministry of Science and Higher Education Grants PBZ/MNiSW/07/2006 and 666/N-CERN/2010/0 and N N202 167440 (1674/B/H03/2011/40) and 1674/B/H03/2011/40.

The author extends her gratitude to the conference committee for the invitation.

## REFERENCES

[1] J. Varela et al. CMS L1 Trigger Control System. *CMS NOTE*, 2002-033, 2002.

[2] W. Adam et al. The CMS high level trigger. *Eur. Phys. J.*, C46:605–667, 2006.

[3] CMS Collaboration. Performance of muon identification in pp collisions at $\sqrt{s} = 7\,TeV$. *CMS PAS MUO*, 10-002, 2010.

[4] CMS Collaboration. Electromagnetic calorimeter commissioning and first result with $7\,TeV$ data. *CMS NOTE*, 2010-012, 2010.

[5] V. Khachatryan et al. Search for Stopped Gluinos in pp collisions at $\sqrt{s} = 7\,TeV$. *Phys. Rev. Lett.*, 106:011801, 2011.

[6] R. Mackeprang and A. Rizzi. Interactions of coloured heavy stable particles in matter. *Eur. Phys. J.*, C50:353–362, 2007.